

This is a repository copy of *Balanced harvesting could reduce fisheries-induced evolution*.

White Rose Research Online URL for this paper:  
<https://eprints.whiterose.ac.uk/137827/>

Version: Accepted Version

---

**Article:**

Law, Richard [orcid.org/0000-0002-5550-3567](https://orcid.org/0000-0002-5550-3567) and Plank, Michael (2018) Balanced harvesting could reduce fisheries-induced evolution. *Fish and fisheries*. pp. 1078-1091. ISSN 1467-2960

---

**Reuse**

Items deposited in White Rose Research Online are protected by copyright, with all rights reserved unless indicated otherwise. They may be downloaded and/or printed for private study, or other acts as permitted by national copyright laws. The publisher or other rights holders may allow further reproduction and re-use of the full text version. This is indicated by the licence information on the White Rose Research Online record for the item.

**Takedown**

If you consider content in White Rose Research Online to be in breach of UK law, please notify us by emailing [eprints@whiterose.ac.uk](mailto:eprints@whiterose.ac.uk) including the URL of the record and the reason for the withdrawal request.

# Balanced harvesting could reduce fisheries-induced evolution

Richard Law, Michael J. Plank

May 31, 2018

Alternative title: On fisheries-induced evolution under balanced harvesting

Running title: Selection and balanced harvesting

Richard Law: York Cross-Disciplinary Centre for Systems Analysis, Ron  
Cooke Hub, University of York, York YO10 5GE, UK

Michael J. Plank: School of Mathematics and Statistics and Te Pūnaha  
Matatini, University of Canterbury, Christchurch, New Zealand

## Abstract

Current fisheries management pays little attention to fisheries-induced evolution. Methods of exploitation that have benefits in the short term, while ameliorating selection in the longer term would therefore be advantageous. Balanced harvesting (BH) is a potential candidate. This tries to bring fishing more in line with natural production, and some short-term benefits for conservation of aquatic ecosystems and for biomass yield have already been documented. It is also predicted to be relatively benign as a selective force on fish stocks, because it keeps the overall distribution of mortality relatively close to natural mortality.

We test this prediction, coupling an ecological model of marine, size-spectrum dynamics to an adaptive-dynamics model of life-history evolution. The evolutionary variable is the reproductive schedule, set by the maximum body mass and the mass at maturation. The prediction is supported by our numerical analysis: directional selection under BH is approximately an order of magnitude weaker than in a standard fishery in which fish experience a fixed rate of fishing mortality after recruitment. The benefit of BH follows from relatively little fishing on large fish, due to the low somatic production rates these big fish have. These results therefore support the general argument for protecting big, old fish, both for ecological and for evolutionary reasons. Slot fisheries that protect large fish share some qualitative features with BH, and show similar evolutionary benefits.

Keywords: adaptive dynamics, ecosystem dynamics, fishing-induced selection, life-history evolution, production rate, size spectrum

# Contents

1. Introduction
2. Theory
  - 2.1 Ecological model
  - 2.2 Evolutionary model
  - 2.3 Strength of directional selection from fishing
3. Numerical results
  - 3.1 Ancestral singular point of evolution
  - 3.2 Patterns of fishing mortality
  - 3.3 Mortality from mackerel predation
  - 3.4 Selection in BH and SAE fisheries
  - 3.5 Selection in slot fisheries
4. Discussion
5. Acknowledgements

# 1 Introduction

Fisheries are potentially important drivers of evolution in fish stocks, because fishing is often a major cause of mortality once fish reach a size at which they are harvested (Heino et al., 2015). There is good evidence for phenotypic change in wild populations consistent with expected effects of fishing, including the much-discussed case of maturation in North East Arctic cod (Eikeset et al., 2016; Enberg and Jørgensen, 2017). There is also experimental evidence that such evolution can take place (Haugen and Vøllestad, 2001; Conover and Munch, 2002; van Wijk et al., 2013). A molecular-genetic basis for such evolution, built on change in gene frequencies at loci linked to traits under selection in the wild, is also being developed (e.g. Chebib et al., 2016).

The precautionary principle calls for the minimization of risks from fisheries-induced evolution (FIE). We are the custodians of marine ecosystems, and responsible for leaving them undamaged for the future. This is enshrined in the Malawi Principle 5 of the Convention on Biological Diversity that motivates the ecosystem-based approach to fisheries management. However, despite the case for evolutionary impact assessment (Jørgensen et al., 2007), the day-to-day reality is that short-term issues of management supercede longer-term issues of FIE (Law, 2007). An example is the plan of the European Union to eliminate discarding of species subject to quota or minimum landing-size regulations in European waters (Common Fisheries Policy reform EU Regulation 1380/2013). This is leading to the development of technical measures that will increase the selectivity of fishing, without consideration of the longer-term consequences for FIE. The short-term solution comes potentially at the cost of exacerbating another, longer-term problem.

One way forward would be to develop methods of fishing that help in the immediate future and, at the same time, ameliorate selection in the longer term (Law, 2007). Balanced harvesting (BH) is a potential candidate for this. BH has been proposed as a way of exploiting fish stocks that would help to maintain the structure and functioning of marine ecosystems, by bringing fishing mortality more in line with the natural production of biomass by species and body sizes (Garcia et al., 2012). For clarity, we define BH at the outset as setting fishing mortality rate to be proportional to the rate of somatic production (dimensions:  $\text{mass vol.}^{-1} \text{ time}^{-1}$ , or  $\text{mass area}^{-1} \text{ time}^{-1}$ ). Perfect BH of an ecosystem is probably unachievable, but it does suggest a direction to go in. The bar for improvement appears to be low: no relationship could be found between fishing mortality rate and production rate of species in a recent study on the West of Scotland shelf ecosystem (Heath et al., 2017). Matters could be improved both by a better

42 balance of fishing mortality across species, and also by a better balance  
43 across body sizes within species. These paths towards a better balance are  
44 complementary, and both could bring fishing more in line with production  
45 rates. Both are the subject of research, including the distribution of fishing  
46 among species or functional groups (Garcia et al., 2012; Kolding et al.,  
47 2016a; Heath et al., 2017), and the distribution of fishing over body sizes  
48 (Law et al., 2012; Jacobsen et al., 2014; Kolding et al., 2016b; Law et al.,  
49 2016).

50 Several short-term benefits of BH have been documented. The open-  
51 access fisheries on the Zambian side of Lake Kariba, with patterns of fishing  
52 mortality closer to BH than the more regulated fisheries of Zimbabwe, give  
53 greater biomass yields with less impact on community structure (Kolding  
54 et al., 2016b). Reducing fishing mortality in species with low production  
55 rate helps to protect those that are rare and vulnerable (Law et al., 2016).  
56 It also reduces ‘longevity overfishing’, aiding the recovery of natural size  
57 structures, by allowing more survival of large individuals (Beamish et al.,  
58 2006). In this way, it improves the resilience of stocks to external pertur-  
59 bations (Hixon et al., 2014).

60 Here we consider a by-product of BH, that could have longer-term ben-  
61 efits of slowing down FIE. This is motivated by models that suggest BH  
62 keeps total mortality within species closer to natural mortality than do  
63 traditional size-at-entry (SAE) fisheries (Law et al., 2015, 2016). A better  
64 alignment between fishing mortality and natural mortality should reduce  
65 selection on the life-histories of fish stocks, and therefore reduce FIE. This  
66 is primarily a prediction about the distribution of fishing mortality over  
67 body size within species, i.e. about BH across body sizes within species,  
68 rather than about BH across species. The purpose of this paper is to test  
69 this prediction about BH. Our numerical results support it. In other words,  
70 BH has an incidental, longer-term advantage of reducing directional selec-  
71 tion from fishing, in addition to its short-term benefits on structure and  
72 functioning of marine ecosystems.

73 To do this work, we developed a method to connect the ecological dy-  
74 namics of size spectra to a simple evolutionary model of adaptive dynamics  
75 (AD) (Kisdi and Geritz, 2010; Brännström et al., 2013). In technical terms,  
76 the work involves analysis of a transversal eigenvalue (the invasion fitness)  
77 of a high-dimensional Jacobian. The Jacobian can be resolved to a simple  
78 form that will allow broader study of evolution in complex, size-structured,  
79 marine ecosystems in the future.

## 80 2 Theory

81 The theory is built in three steps (Fig. 1). (Step 1) An ecological model  
82 of the dynamics of coupled size spectra: this is needed because there is no  
83 external notion of fitness in an AD model—fitness of genetically distinct  
84 phenotypes emerges directly from the ecological processes. (Step 2) An  
85 evolutionary model based on AD within which the ecological dynamics are  
86 nested: this moves an ancestral population through a sequence of muta-  
87 tion and selection events, driven by predation in the size spectra, leading  
88 eventually to a singular point at which there is no further evolution. The  
89 system is then at an evolutionarily stable state (ESS), before fishing is  
90 added. Without a separation of this kind, selection from fishing would be  
91 conflated with selection from predation taking place inside the food web.  
92 (Step 3) Calculation of the strength and direction of selection generated by  
93 a range of patterns of fishing at the ESS.

94 FIGURE 1 NEAR HERE

### 95 2.1 Ecological model

96 Dynamic size-spectrum models of marine ecosystems couple together an  
97 arbitrary number of species through size-dependent feeding (Andersen and  
98 Beyer, 2006; Hartvig et al., 2011; Blanchard et al., 2014; Jacobsen et al.,  
99 2014). Like any model of a complex, real-world marine ecosystems, they  
100 are a simplification. However, they are built up from realistic assumptions  
101 about the frequency of predator-prey interactions between individuals of  
102 a given size (Andersen et al., 2016). First, they assume that body size  
103 is the primary driver of the trophic level at which marine organisms feed.  
104 This property of marine trophic structure is in keeping with empirical re-  
105 search on stable isotopes of nitrogen (Jennings et al., 2001). Second, they  
106 deal explicitly with the growth of individuals as they eat other smaller or-  
107 ganisms, so there is no external growth model, such as a von Bertalanffy  
108 growth equation. Third, they assume that the most common cause of death  
109 is through being eaten by larger organisms, which leaves less uncertainty  
110 about rates of natural mortality. Fourth, they assume that species are  
111 coupled through the body-size dependence of their prey: they are both  
112 predators on other species, and cannibals on themselves. Different species  
113 clearly can specialise in ways that affect their locations in food webs, and  
114 size-spectrum models incorporate some species-dependent feeding param-  
115 eters. Importantly, unlike most models in fisheries science, size-spectrum  
116 models do the bookkeeping of biomass flowing in and out of species and  
117 size categories, as individuals eat one another and grow (e.g. Law et al.,

118 2016).

119 The state variables of size-spectrum models are functions that describe  
 120 the density of organisms  $\phi_i(w, t)$  as functions of body mass  $w$  and time  $t$ ,  
 121 where  $i$  is an index for species. The core of such a model is a system of par-  
 122 tial differential equations (PDEs), one equation for each species, describing  
 123 how the density function  $\phi_i(w, t)$  of each species unfolds over time through  
 124 feeding (and consequent growth, reproduction and death). At their sim-  
 125 plest, the PDEs take the form of a McKendrick—von Foerster equation,  
 126 with body mass rather than age being the independent variable (Sinko and  
 127 Streiffer, 1971; Silvert and Platt, 1978):

$$128 \quad \frac{\partial}{\partial t} \phi_i = - \overbrace{\frac{\partial}{\partial w} [\tilde{g}_i \phi_i]}^{(a)} - \overbrace{\tilde{\mu}_{\text{tot}, i} \phi_i}^{(b)}. \quad (2.1)$$

129 To help understand this equation, Fig. 2 shows the meaning of terms on the  
 130 right-hand side. Term (a) describes the change in density at body mass  $w$ ,  
 131 due to feeding on smaller fish, contained in the function  $\tilde{g}_i(w, t)$  the growth  
 132 rate of individuals of body mass  $w$  at time  $t$ . This is calculated as a function  
 133 of the abundance of smaller, conspecific and heterospecific individuals, of a  
 134 suitable size to be prey of a individual of body mass  $w$ . Term (b) describes  
 135 the change in density at body mass  $w$ , due to death;  $\tilde{\mu}_{\text{tot}, i}(w, t)$  is the total  
 136 per capita death rate for individuals of body mass  $w$ . This is calculated  
 137 as a function of the abundance of larger, conspecific and heterospecific  
 138 individuals of a suitable size to be predators of an individual of body mass  
 139  $w$  at time  $t$ , plus other sources of mortality including sensesence and fishing.  
 140 See Appendix A for full mathematical details.

141 FIGURE 2 NEAR HERE

142 In addition to species-dependent feeding, multispecies size spectra allow  
 143 species to have different life histories. Life-history parameters include, for  
 144 instance, the asymptotic body mass  $w_{i, \infty}$ , and body mass at 50 % mat-  
 145 uration  $w_{i, m}$ . In non-seasonal, size-spectrum models, individuals allocate  
 146 an increasing proportion of incoming biomass towards reproduction and  
 147 away from somatic growth as they mature, the proportion reaching 1 at  
 148  $w_{i, \infty}$  where somatic growth ends. For a given egg size, this is enough to  
 149 define a schedule of reproduction at the level of species. Predation mor-  
 150 tality and growth, which are also components of the life history, are not  
 151 set as externalities in size-spectrum models, as they emerge from size- and  
 152 density-dependent feeding in the food web. However, some additional death  
 153 is incorporated, recognising that predation is not the only reason why or-  
 154 ganisms die, and such death may include mortality from fishing. In this  
 155 way the life history is defined at the species level.



156 Note that the smallest organisms must have food to eat if they are to  
157 grow, so size spectra have to be extended down into the spectrum of uni-  
158 cellular plankton. For simplicity, we used a fixed plankton spectrum, set to  
159 values that correspond approximately to those observed. This is equivalent  
160 to an assumption that the plankton dynamics happen on a faster timescale  
161 and cannot be exhausted by predation, and it has the effect that fish popu-  
162 lation growth is not limited by the plankton. However, the predation and  
163 cannibalism among the fish are enough to hold their population growth in  
164 check, as long as the upper limit of plankton body size is kept sufficiently  
165 small relative to the sizes of maturation in the fish species.

## 166 2.2 Evolutionary model

167 We used adaptive dynamics (AD) to describe phenotypic evolution. AD  
168 was developed in the 1990s to provide a direct link between population  
169 dynamics and phenotypic evolution (Kisdi and Geritz, 2010). The basic  
170 dynamics and their graphical representation were given in some early pa-  
171 pers (Metz et al., 1992; Dieckmann and Law, 1996; Metz et al., 1996; Geritz  
172 et al., 1998), and a review by Brännström et al. (2013) gives an overview  
173 of the subject. The idea is that phenotypic traits, such as asymptotic  
174 body mass  $w_{i,\infty}$ , although fixed in ecological time, have a genetic com-  
175 ponent that is under selection driven directly by the ecological processes.  
176 In the context of multispecies size spectra, AD allows evolution of traits  
177 to emerge from natural selection generated by the multispecies food web  
178 without simplifying the ecology. There is a cost to this in terms of certain  
179 assumptions, the most important being a time-scale separation between the  
180 ecological and evolutionary dynamics: mutations to the trait have to be  
181 infrequent enough for the food web to be at its asymptotic state (typically  
182 an equilibrium point) before the next mutant appears. Other assumptions  
183 to make the dynamics more tractable include small mutational steps, a  
184 simple asexual mutation-selection process (a trait-substitution sequence),  
185 and populations that are dominated by a single phenotype at each step.

186 The path of evolution is determined by the initial rate of increase (in-  
187 vasion fitness) of mutants as they arise in the resident food web. An evo-  
188 lutionary step starts with the ecological system running to its asymptotic  
189 state with a set of resident trait values  $\mathbf{s}$  for the species. Having reached  
190 this state, a function  $\lambda_i(s'_i, \mathbf{s})$  defines the invasion fitness of a mutant with  
191 an altered trait value  $s'_i$  in species  $i$ . Despite the complexity of the resident  
192 food web, the eigenvalue corresponding to the invasion fitness is found rel-  
193 atively easily from a Jacobian matrix that contains the mutant dynamics  
194 Eq. (B.1) (Appendix B). Evolution of the set of traits is then given by a

195 system of canonical equations, with one equation for each evolving species:

$$196 \quad \frac{ds_i}{dt} = k_i \frac{\partial}{\partial s'_i} \lambda_i(s'_i, \mathbf{s}) \Big|_{s'_i=s_i} \quad (2.2)$$

197 (Dieckmann and Law, 1996), where  $k_i$  is an evolutionary rate constant for  
 198 species  $i$ . The core information about selection is carried by the partial  
 199 derivative of the invasion fitness in the direction of the mutant when the  
 200 mutant is rare (the selection gradient). What happens if the mutant in-  
 201 creases would seem to be left unanswered by this, but a theorem gives the  
 202 conditions under which invasion implies fixation of the mutant, and these  
 203 conditions apply quite widely (Geritz et al., 2002).

## 204 2.3 Strength of directional selection from fishing

205 To examine some basic effects of selective fishing we took just two interact-  
 206 ing fish species from the general framework above, and allowed evolution of  
 207 one trait on one of them. The evolving trait was the asymptotic body mass  
 208  $w_\infty$ , and the mass at 50 % maturation  $w_m$  was assumed to be a fixed pro-  
 209 portion of this, so that the whole reproductive schedule would move with  
 210 body size as the trait evolved. This is in keeping with the similar length ra-  
 211 tios  $l_m/l_\infty$  observed in similar-shaped fish species, in taxonomically related  
 212 fish species, and in different populations of single species, despite substan-  
 213 tial variation in  $l_\infty$  (Beverton, 1992; Froese and Binohlan, 2000). (As only  
 214 one species is evolving, the species index is omitted below.)

215 In an evolving system as simple as this, the invasion-fitness surface  
 216  $\lambda(w'_\infty, w_\infty)$  is enough to show the qualitative outcome of evolution. An  
 217 example is given in Fig. 3: the surface is saddle-like, and has a singular  
 218 point of evolution  $w_\infty^*$  at which the selection gradient in Eq. (2.2) is zero.  
 219 The singular point can be seen by taking a section through through the  
 220 surface at  $\lambda = 0$  known as the pairwise invasibility plot (PIP) (Fig. 3); the  
 221 singular point is at the intersection of the two lines (Geritz et al., 1998;  
 222 Brännström et al., 2013). In the system described below, the asymptotic  
 223 mass evolved to this point and came to rest there. Thus, in this instance,  
 224 the singular point is a continuously stable strategy (CSS), i.e. an evolu-  
 225 tionarily stable strategy (ESS) (Smith and Price, 1973), to which there  
 226 is convergence through evolution (Geritz et al., 1998; Brännström et al.,  
 227 2013). We take  $w_\infty^*$  as the trait value of the evolved ancestral population,  
 228 prior to the introduction of fishing.

229 FIGURE 3 NEAR HERE

230 When fishing mortality is added, the shape of the invasion-fitness surface  
 231 is distorted, and the singular point at  $w_\infty^*$  becomes invadable by mutants.

Some examples are shown in Fig. 4a. The gradient at  $w_\infty^*$  clearly depends on the fishing mortality, and shows the strength of selection generated by fishing. Thus we measure the strength of directional selection  $S$  as the slope at the singular point  $w_\infty^*$ :

$$S = \frac{\partial}{\partial \log w'_\infty} \lambda(w'_\infty, w_\infty) \Big|_{w'_\infty = w_\infty^*}, \quad (2.3)$$

to compare the selective effects of different patterns of exploitation below. (Fig. 3 shows the direction along which the slope is measured.) If the slope becomes negative when fishing is introduced, mutants with smaller  $w_\infty$  can invade, and those with larger  $w_\infty$  cannot; steeper this slope, the greater the selective advantage of these mutants.

In due course, a new mortality regime would cause evolution to another phenotypic state. However, it would be inadvisable to use a simple AD model to investigate this. The strong selection generated by fishing would violate the time-scale separation between ecological and evolutionary dynamics assumed in the AD model. Other methods avoiding this assumption would be preferred, such as quantitative-genetic and ecogenetic models (Andersen and Brander, 2009; Dunlop et al., 2009). AD in this paper is used just to construct an ancestral singular point of evolution, and to measure the strength of selection generated by patterns of fishing mortality at that singular point.

FIGURE 4 NEAR HERE

## 3 Numerical results

### 3.1 Ancestral singular point of evolution

For numerical analysis, we took an ecological system similar to that of Law et al. (2016), comprising a fixed plankton spectrum, together with two fish species, one growing to a small size, and the other to a large size (notionally mackerel and cod). The parameter values specifying the ecological system are given in Appendix C. Some effects of different fishing regimes on this and simpler systems in the absence of evolution have been shown in earlier papers (Law et al., 2015, 2016), but an evolutionary model is needed to examine the strength of selection generated by different fishing methods.

Cod was taken as the evolving species, and the evolving trait was  $w_\infty$  with the 50 % maturation as a fixed proportion,  $1/15$  of  $w_\infty$ . A singular point of evolution of the ancestral cod was found at  $w_\infty^* \approx 85$  kg (Fig. 3),

near the size of the largest cod ever recorded (Kolding personal communication). Equivalently, mass at 50 % maturity  $w_m^*$  was 5.67 kg. Predation by mackerel on small cod was the main driver of late maturation in cod in our numerical model, and the strength of predation was therefore tuned to obtain the ancestral value (Appendix C). (In the absence of mackerel, evolution of the ancestral cod would bring cod to a singular point of evolution at  $w_\infty^* = 27$  kg in our numerical analysis (results not shown).) The large asymptotic mass and longevity of ancestral cod can be interpreted as an evolutionary outcome of the escape that this gives from heavy predation early in life (Williams, 1966, p.89-91).

The invulnerability of the ancestral cod at  $w_\infty^* \approx 85$  kg in the absence of fishing is evident from the section through the invasion-fitness surface in the direction of the mutant at  $w_\infty^*$  (Fig. 4a, heavy dotted curve). This line reaches its maximum value of zero at  $w_\infty^*$ : in other words,  $w_\infty^*$  is an ESS, uninvadable by any mutant with another trait value  $w'_\infty$  in its neighbourhood. The point  $w_\infty^*$  is taken as the state to which cod evolved prior to the introduction of fishing.

### 3.2 Patterns of fishing mortality

We considered three ways in which to distribute fishing mortality rate over body size (Fig. 5). (1) Balanced harvesting (BH) sets the rate to be proportional to the current rate of somatic production at each size, from some minimum size of capture onwards (see Appendix D). (2) Size-at-entry (SAE) fishing has a minimum capture size above which the fishing mortality is constant irrespective of body size. (3) Slot fishing has constant fishing mortality like SAE, but has an additional a maximum body size above which fish are not caught. Each fishing pattern has a parameter controlling the overall intensity of fishing. Under SAE and slot fishing, this is the fishing mortality rate,  $F$ , within the exploited size range. Under BH,  $F$  is a function of body size, and the parameter is a constant of proportionality  $c$  (units:  $\text{m}^3 \text{g}^{-1}$ ) between the production rate and the fishing mortality at a given body mass.

FIGURE 5 NEAR HERE

Thus the fishing patterns differ in the fishing mortality above some minimum size of capture (assumed to be knife-edge). Notice that the fall in somatic growth rate and biomass, which typically happens when fish become large for their species, has the effect of making the somatic production rate decrease. This is therefore accompanied by a corresponding fall in fishing mortality under BH. The different fishing patterns distort the

invasion-fitness surface (Fig. 3) in different ways, generating different selection gradients, which will be described below.

The key to understanding the selection on cod generated by fishing is through the changing regime of mortality on cod that fishing brings about. This comes in two parts. First, there is a direct effect on mortality from the fish that are caught. Second, hidden beneath this, are changes in intrinsic mortality, predation mortality and cannibalism inside the size-structured food web, as it adjusts to the fishing. The ecological size-spectrum dynamics automatically keep track of these internal changes, and the effects of the changes are felt by non-target as well as by target species.

### 3.3 Mortality from mackerel predation

The hidden effects of predation are important. For instance, mackerel is not a passive partner in the evolution of cod: predation by mackerel is part of the mortality experienced by cod. If mackerel are harvested, the predation by mackerel on cod is reduced, and this leaves a footprint on the invasion fitness of mutants  $w'_\infty$  in cod, favouring those with lower  $w'_\infty$  (Fig. 4a, dash-dot line), irrespective of any fishing on cod.

We assumed a fixed background of fishing on mackerel, harvested as a SAE fishery with a fishing mortality rate  $0.5 \text{ yr}^{-1}$  starting at a body mass 250 g. We did this because cod could be seriously depleted by the combined effects of heavy fishing and predation from mackerel, if the latter was unexploited. So fishing on mackerel here was taken as a fixed part of the environment of cod, and was not balanced to match fishing on cod (cf. Law et al., 2016). The selection gradients on cod under fishing should therefore be taken relative to the selection gradient on cod already caused by catching mackerel. However, the impact on cod of fishing mackerel at this level is relatively small, as shown in Fig. 4a.

### 3.4 Selection in BH and SAE fisheries

A BH fishery on cod leads to much less selection on the life history than a SAE fishery (Fig. 4a: continuous and dashed lines). This can be seen from the much steeper gradient in the invasion fitness under SAE (continuous curve) than under BH (dashed curve), and is consistent with the prediction that BH is relatively benign in its effects on FIE. Depending on whether the selective effect of fishing mackerel is allowed for, the selection gradient in the SAE fishery is from about five to twenty times that in the BH fishery at the same biomass yield. Fig. 4b extends the comparison of BH and SAE

340 fisheries to show the relation between selection gradient and biomass yield  
 341 as cod fishing mortality increases from zero (the fishing mortality rate on  
 342 mackerel is fixed throughout). The major benefits from BH in reducing  
 343 selection are clear. Note that the selection gradient on cod is negative even  
 344 when there is no fishing on cod, because mackerel fishing automatically  
 345 changes the pattern of predation on cod.

346 Fig. 6 gives a sensitivity analysis of the effect of varying fishing pressure  
 347 over a range of minimum capture sizes. This confirms the much weaker se-  
 348 lection in BH than in SAE fisheries as the minimum capture size is varied:  
 349 for a given biomass yield, the selection gradient is substantially closer to  
 350 zero in BH than in SAE fishing. Yield rises to a peak as fishing increases  
 351 and then falls until extinction occurs. BH gives the greatest benefits to re-  
 352 ducing selection with moderate levels of fishing, well before the maximum  
 353 yield is reached. The yield does not return smoothly to zero as fishing  
 354 increases; instead there is a threshold when the combined effects of fish-  
 355 ing, cannibalism, and predation by mackerel reach a point at which cod  
 356 collapses.

357 **FIGURE 6 NEAR HERE**

358 The main benefit of BH comes from bringing fishing in line with pro-  
 359 duction rates of large (not small) fish. This is evident from the fact that  
 360 the minimum capture sizes in the BH fisheries in Fig. 6a have relatively  
 361 little effect on the selection gradients as the biomass yield is growing. In  
 362 contrast, in the SAE fisheries (Fig. 6b), selection for earlier maturation  
 363 becomes stronger (i.e.,  $S$  becomes more negative), as fishing becomes more  
 364 concentrated on adults. In the BH fisheries, the selection gradients in fact  
 365 get slightly closer to zero as the minimum capture size increases (Fig. 6a),  
 366 thereby countering the effect of mackerel fishing.

### 367 **3.5 Selection in slot fisheries**

368 A detailed balancing of fishing to production rate by species and body size  
 369 would be hard to achieve in practice. Evidently, low fishing mortality on  
 370 the big fish that have low production rates is the key to reducing fisheries-  
 371 induced selection on the reproduction schedule. We therefore examined the  
 372 sensitivity of selection to a range of slot fisheries, as a first approximation  
 373 to BH (Fig. 7), using two fixed ratios of maximum/minimum capture  
 374 size of 5 and 10. Like BH and SAE, the yield rises to a peak as fishing  
 375 increases. But unlike BH, the extinction point can be close to the peak  
 376 unless the minimum capture size is large. Since collapse could occur with  
 377 little warning, slot fisheries on small fish would need to be implemented

378 with care.

379 FIGURE 7 NEAR HERE

380 The effect of sliding the slot fisheries across the life history of cod is  
381 consistent with a basic notion of life-history theory, that organisms evolve  
382 to avoid states where they are at their most vulnerable (Williams, 1966).  
383 When small cod are caught (minimum capture sizes: 30, 100, 300 g), the  
384 ancestral advantage in large body size as an escape from predation weakens  
385 and, as in BH, relatively weak selection for earlier maturation occurs. Such  
386 fishing is undoing part of the ancestral selection pressure for late maturation.  
387 When intermediate-sized cod are caught (minimum capture size: 1  
388 kg), delayed maturation allows faster growth through the vulnerable size  
389 range, pushing the selection gradient a little in the opposite direction, even  
390 to the point of reversing the direction of selection (Fig. 7b). When large  
391 cod are caught (minimum capture size: 3 kg), delaying maturation carries  
392 the heavy cost of potentially not reproducing at all, and, as in SAE fishing,  
393 there is strong selection for early maturation.

394 The reversal of fisheries-induced selection is remarkable (Fig. 7b, fishing  
395 from 1 to 10 kg). We interpret it in part as an interaction with the mackerel  
396 fishery, since this slot size range would include cod that would otherwise  
397 be eating the exploited size range of mackerel to a major degree. Catching  
398 these cod thus allows more of these mackerel to escape predation, despite  
399 the fishery on them (and also more escape from predation by cod of a  
400 similar size). The outcome is heavier predation on cod still earlier in life,  
401 and overall selection for later maturation.

## 402 4 Discussion

403 Our results support the prediction that BH is a good deal more benign  
404 than traditional SAE fisheries as a selective pressure on the life histories of  
405 fish. This is contingent on fishing mortality being set at a moderate level.  
406 Although the ecological context of multispecies size spectra is different from  
407 previous work, the basic feature, that organisms evolve not to linger in  
408 vulnerable states, is congruent with earlier work on life-history evolution  
409 (Williams, 1966; Edley and Law, 1988), suggesting a robustness of the  
410 results that goes beyond particular model structures. The simple message  
411 is that, to keep fishing-induced selection small, it helps to protect big fish  
412 with low production rates.

413 Importantly, BH is as much about *reducing* fishing on components of  
414 ecosystems that have low production, as it is about fishing on those that

415 have high production. Fish that are big for their species typically have  
 416 relatively low somatic production rates, (a) because they have low mass-  
 417 specific somatic growth rates, and (b) because a history of fishing tends to  
 418 truncate size structures, leaving the remaining big fish with low biomass  
 419 densities. The somatic production rate is simply the product (a)  $\times$  (b),  
 420 and BH therefore calls for correspondingly little fishing on these big fish.  
 421 BH thus aligns with a major stream of thinking that big, old fish need  
 422 protection both for ecological and for evolutionary reasons (Beamish et al.,  
 423 2006; Hsieh et al., 2006, 2010; Hixon et al., 2014). BH contributes to this  
 424 literature in suggesting somatic production rate as a quantitative guide for  
 425 setting relative levels of fishing mortality.

426 A precise balancing of fishing mortality to production rate by body  
 427 size would be hard to achieve in practice. Slot fisheries that select an  
 428 intermediate range of body size resemble BH at a qualitative level, as they  
 429 create a refuge for large fish. Our results on fisheries-induced selection  
 430 caused by slot fishing are consistent with those of a recent study on the  
 431 use of gillnets in NE Arctic cod (Zimmermann and Jørgensen, 2017). Slot  
 432 fishing deserves attention in the drive for increased selectivity to reduce  
 433 discarding (Common Fisheries Policy reform EU Regulation 1380/2013).  
 434 Selectivity *per se* is not the issue—it is what is being selected that matters.  
 435 To get the evolutionary benefits from slot fisheries, their upper limits should  
 436 not extend too far into adult life, as that would generate a strong selective  
 437 advantage for early reproduction. Slot fisheries involving juveniles have to  
 438 be implemented with caution because of the clear danger that stocks could  
 439 collapse from over-exploitation.

440 Taking a multispecies, size-spectrum model as the ecological input into  
 441 a model of AD provides a new route into life-history evolution and FIE. It  
 442 deals internally with all the density-dependent growth and mortality gener-  
 443 ated by predation and cannibalism in the size-structured, food-web model.  
 444 In this way, it removes an artificial separation of natural mortality from  
 445 fishing mortality. This has some interesting consequences. For instance,  
 446 it shows how fishing on one species generates selection on another (unex-  
 447 ploited) species, as the food web adjusts to the fishing. It also shows that a  
 448 fishing regime, appropriately chosen, could change the predation mortality  
 449 generated within the food-web, reversing the direction of selection caused  
 450 by fishing. This would be system specific, and would require a detailed un-  
 451 derstanding of how the food web works. The framework we have developed  
 452 offers a route to exploring the selection pressures generated by fishing on  
 453 multiple species within a marine ecosystem.

454 Quite apart from the context of FIE, coupling size-spectrum dynamics to  
 455 AD should facilitate research into broader issues about evolution in aquatic



456 food webs. Current models of size spectrum dynamics contain a number of  
457 parameters that could be evolutionary variables, such as how far down the  
458 food web predators are feeding, how broad their diets are, and how active  
459 they are. Further ecological parameters are likely to become part of the  
460 language of size-spectrum models as the research field develops, and AD  
461 provides a flexible framework for studying their evolution.

462 One general evolutionary issue is whether there is a simple maximisation  
463 principle at work. Such a principle, that species evolve to reproduce at the  
464 body size at which cohort biomass is greatest, has been suggested  
465 by Froese et al. (2016) as an argument for the implausability of peaks in  
466 biomass at small body size (Law et al., 2016). Our evolutionary analysis  
467 does not support this maximum-biomass principle: irrespective of biomass  
468 peaks, predation by mackerel on small cod generates an advantage for late  
469 maturation in cod. Peaks and troughs in cohort biomass (and equivalently  
470 somatic production rate) occur at body sizes where mass-specific growth  
471 rate and death rate intersect (Law et al., 2016, Appendix E). These rate  
472 functions are nonlinear and rather labile as they are strongly affected by  
473 the prevailing predation in the food web. We would therefore expect the  
474 peaks of cohort biomass to move around during the course of evolution.  
475 Until more is known about such evolution, it is probably sensible to keep  
476 an open mind about where peaks in cohort biomass are located with respect  
477 to body size, and to try to understand more about the location of peaks  
478 from empirical work.

479 Among the caveats about this study is the reduction of the life history  
480 to a single scalar measure of reproduction, to allow the whole reproduction  
481 schedule to shift to smaller or larger body sizes. This allows some basic  
482 calculations, but it simplifies the multidimensional, phenotypic structure of  
483 the life history. For instance, there is special interest in probabilistic matu-  
484 ration reaction norms (PMRNs) as sensitive indicators of FIE (Heino et al.,  
485 2002; Heino and Dieckmann, 2008). The ecological, size-spectrum dynam-  
486 ics do carry dependence of growth on food, so there is an implied PMRN,  
487 which would be seen as prey densities change; this PMRN would depend  
488 on age (not body size) with the size-spectrum model as implemented here.

489 A second caveat is that we have not dealt with the rate at which FIE  
490 takes place. This is because it would be hard to justify AD's time-scale  
491 separation between ecological and evolutionary dynamics in contemporary  
492 fisheries. Our results say only that, for a given biomass yield, the strength  
493 of selection could be brought down by roughly an order of magnitude by  
494 moving from SAE fishing to BH and appropriate slot fisheries. The rate of  
495 evolutionary change caused by fishing is widely discussed (e.g. Jørgensen  
496 et al., 2007; Andersen and Brander, 2009; Audzijonyte et al., 2013a; Heino

et al., 2015), but has not gained traction in the practical management of fisheries. This is unfortunate because the longer, decadal time-scale of FIE does not absolve managers of marine ecosystems from responsibility for such changes. One reason for linking FIE to BH is that, as well as helping to resolve some short-term issues, BH can evidently also assist conservation of fish stocks in the longer term.

A third caveat is that fishing gear obviously has many selective effects other than changing the mortality rate, for instance on behaviour or reproductive phenology (Heino et al., 2015; Andersen et al., 2018; Tillotson and Quinn, 2018). Such selective effects of fishing gear can be quite different from those generated by natural predators. The prediction in this paper is simply about the distribution of mortality on the evolution of life histories under different schemes of fishing.

Our main result, that fisheries-induced selection would be reduced by lowering fishing mortality on fish that are big for their species, should be robust. However the fine details of feedbacks within food webs are bound to be context dependent. Feedbacks in multispecies, size-structured food webs are intricate, and the challenge as fisheries science moves towards an ecosystem approach is to see what, if any, broad robust patterns emerge from the fine details (Audzijonyte et al., 2013b).

## Acknowledgements

This research received funding from the European Commissions Horizon 2020 Research and Innovation Programme under Grant Agreement No. 634495 for the project Science, Technology, and Society Initiative to minimize Unwanted Catches in European Fisheries (MINOUW). MJP was partly funded by Te Pūnaha Matatini, a New Zealand Centre of Research Excellence. The work was facilitated by the School of Mathematics and Statistics, University of Canterbury, New Zealand, which hosted a research visit by RL. Gustav Delius and Richard Southwell gave advice on implementing the fast Fourier transform.

## References

- Andersen, K. H. and Beyer, J. E. (2006). Asymptotic size determines species abundance in the marine size spectrum. *American Naturalist*, 168:54–61.
- Andersen, K. H., Blanchard, J. L., Fulton, E. A., Gislason, H., Jacobsen, N. S., and van Kooten, T. (2016). Assumptions behind size-based ecosystem models are realistic. *ICES Journal of Marine Science*, 73:1651–1655. doi:10.1093/icesjms/fsv211.
- Andersen, K. H. and Brander, K. (2009). Expected rate of fisheries-induced evolution is slow. *Proceedings of the National Academy of Sciences USA*, 106:11657–11660. doi:10.1073/pnas.0901690106.
- Andersen, K. H., Marty, L., and Arlinghaus, R. (2018). Evolution of boldness and life history in response to selective harvesting. *Canadian Journal of Fisheries and Aquatic Sciences*, 75:271–281. dx.doi.org/10.1139/cjfas-2016-0350.
- Audzijonyte, A., Kuparinen, A., and Fulton, E. A. (2013a). How fast is fisheries-induced evolution? quantitative analysis of modelling and empirical studies. *Evolutionary Applications*, 6:585–595. doi:10.1111/eva.12044.
- Audzijonyte, A., Kuparinen, A., Gorton, R., and Fulton, E. A. (2013b). Ecological consequences of body size decline in harvested fish species: positive feedback loops in trophic interactions amplify human impact. *Biology Letters*, 9:20121103. doi:10.1098/rsbl.2012.1103.
- Beamish, R. J., McFarlane, G. A., and Benson, A. (2006). Longevity overfishing. *Progress in Oceanography*, 68:289–302. doi:10.1016/j.pocean.2006.02.005.
- Beverton, R. J. H. (1992). Patterns of reproductive strategy parameters in some marine teleost fishes. *Journal of Fish Biology*, 41 (Supplement B):137–160. doi.org/10.1111/j.1095-8649.1992.tb03875.x.
- Blanchard, J. L., Andersen, K. H., Scott, F., Hintzen, N. T., Piet, G., and Jennings, S. (2014). Evaluating targets and trade-offs among fisheries and conservation objectives using a multispecies size spectrum model. *Journal of Applied Ecology*, 51:612–622. doi:10.1111/1365-2664.12238.
- Brännström, Å., Johansson, J., and von Festenberg, N. (2013). The hitchhikers guide to adaptive dynamics. *Games*, 4:304–328. doi:10.3390/g4030304.

- 563 Chebib, J., Renaut, S., Bernatchez, L., and Rogers, S. M. (2016). Genetic  
564 structure and within-generation genome scan analysis of fisheries-induced  
565 evolution in a lake whitefish (*Coregonus clupeaformis*) population. *Con-*  
566 *servation Genetics*, 17:473–483. doi:10.1007/s10592-015-0797-y.
- 567 Conover, D. O. and Munch, S. B. (2002). Sustaining fisheries yields over  
568 evolutionary time scales. *Science*, 297:94–96.
- 569 Datta, S., Delius, G. W., and Law, R. (2010). A jump-growth  
570 model for predator-prey dynamics: derivation and application to ma-  
571 rine ecosystems. *Bulletin of Mathematical Biology*, 72:1361–1382.  
572 doi:10.1007/s11538-009-9496-5.
- 573 Datta, S., Delius, G. W., Law, R., and Plank, M. J. (2011). A stability  
574 analysis of the power-law steady state of marine size spectra. *Journal of*  
575 *Mathematical Biology*, 63:779–799. doi:10.1007/s00285-010-0387-z.
- 576 Dieckmann, U. and Law, R. (1996). The dynamical theory of coevolution: a  
577 derivation from stochastic ecological processes. *Journal of Mathematical*  
578 *Biology*, 34:579–612.
- 579 Dunlop, E. S., Heino, M., and Dieckmann, U. (2009). Eco-genetic modeling  
580 of contemporary life-history evolution. *Ecological Applications*, 19:1815–  
581 1834.
- 582 Edley, M. T. and Law, R. (1988). Evolution of life histories and yields in  
583 experimental populations of *Daphnia magna*. *Biological Journal of the*  
584 *Linnean Society*, 34:309–326.
- 585 Eikeset, A. M., Dunlop, E. S., Heino, M., Storvik, G., Stenseth, N. C.,  
586 and Dieckmann, U. (2016). Roles of density-dependent growth and life  
587 history evolution in accounting for fisheries-induced trait changes. *Pro-*  
588 *ceedings of the National Academy of Sciences USA*, 113:15030–15035.  
589 doi:10.1073/pnas.1525749113.
- 590 Enberg, K. and Jørgensen, C. (2017). Conclusion that fishing-induced  
591 evolution is negligible follows from model assumptions. *Proceedings of the*  
592 *National Academy of Sciences USA*, 114:. doi:10.1073/pnas.1700708114.
- 593 Froese, R. and Binohlan, C. (2000). Empirical relationships to estimate  
594 asymptotic length, length at first maturity and length at maximum yield  
595 per recruit in fishes, with a simple method to evaluate length frequency  
596 data. *Journal of Fish Biology*, 56:758–773. doi:10.1006/jfbi.1999.1194.

- 597 Froese, R., Walters, C., Pauly, D., Winker, H., Weyl, O. L. F., Demirel, N.,  
598 Tsikliras, A. C., and Holt, S. J. (2016). A critique of the balanced har-  
599 vesting approach to fishing. *ICES Journal of Marine Science*, 73:1640–  
600 1650. doi:10.1093/icesjms/fsv122.
- 601 Garcia, S. M., Kolding, J., Rice, J., Rochet, M.-J., Zhou, S., Arimoto,  
602 T., Beyer, J. E., Borges, L., Bundy, A., Dunn, D., Graham, N., Hall,  
603 M., Heino, M., Law, R., Makino, M., Rijnsdorp, A. D., Simard, F., and  
604 Smith, A. D. M. (2012). Reconsidering the consequences of selective  
605 fisheries. *Science*, 335:1045–1047.
- 606 Geritz, S. A. H., Gyllenberg, M., Jacobs, F. J. A., and Parvinen, K. (2002).  
607 Invasion dynamics and attractor inheritance. *Journal of Mathematical*  
608 *Biology*, 44:560–560. doi:10.1007/s002850100136.
- 609 Geritz, S. A. H., Kisdi, É., Meszéna, G., and Metz, J. A. J. (1998). Evo-  
610 lutionarily singular strategies and the adaptive growth and branching of  
611 the evolutionary tree. *Evolutionary Ecology*, 12:35–57.
- 612 Hartvig, M., Andersen, K. H., and Beyer, J. E. (2011). Food web framework  
613 for size-structured populations. *Journal of Theoretical Biology*, 272:113–  
614 122. doi:10.1016/j.jtbi.2010.12.006.
- 615 Haugen, T. O. and Vøllestad, L. A. (2001). A century of life-history evo-  
616 lution in grayling. *Genetica*, 112113:475–491.
- 617 Heath, M., Law, R., and Searle, K. (2017). Scoping the background in-  
618 formation for an ecosystem approach to fisheries in scottish waters: Re-  
619 view of predator-prey interactions with fisheries, and balanced harvest-  
620 ing. Technical report, A study commissioned by Fisheries Innovation  
621 Scotland (FIS). ISBN: 978-1-911123-10-1, www.fiscot.org.
- 622 Heino, M. and Dieckmann, U. (2008). Detecting fisheries-induced life-  
623 history evolution: an overview of the reaction norm approach. *Bulletin*  
624 *of Marine Science*, 83:69–93.
- 625 Heino, M., Dieckmann, U., and Godø, O. R. (2002). Measuring probabilis-  
626 tic reaction norms for age and size at maturation. *Evolution*, 56:669–678.
- 627 Heino, M., Pauli, B. D., and Dieckmann, U. (2015). Fisheries-induced  
628 evolution. *Annual Review of Ecology and Systematics*, 46:461–480.  
629 doi:10.1146/annurev-ecolsys-112414-054339.
- 630 Hixon, M. A., Johnson, D. W., and Sogard, S. M. (2014). BOFFFFs:  
631 on the importance of conserving old-growth age structure in fish-  
632 ery populations. *ICES Journal of Marine Science*, 73:1623–1631.  
633 doi:10.1093/icesjms/fst200.

- 634 Hsieh, C.-h., Reiss, C. S., Hunter, J. R., Beddington, J. R., May, R. M.,  
635 and Sugihara, G. (2006). Fishing elevates variability in the abundance  
636 of exploited species. *Nature*, 443:859–862. doi:10.1038/nature05232.
- 637 Hsieh, C.-h., Yamauchi, A., Nakazawa, T., and Wang, W.-F. (2010). Fish-  
638 ing effects on age and spatial structures undermine population stability  
639 of fishes. *Aquatic Sciences*, 72:165–178. doi:10.1007/s00027-009-0122-2.
- 640 Jacobsen, N. S., Gislason, H., and Andersen, K. H. (2014). The conse-  
641 quences of balanced harvesting of fish communities. *Proceedings of the*  
642 *Royal Society B*, 281:20132701. doi:0.1098/rspb.2013.2701.
- 643 Jennings, S., Pinnegar, J. K., Polunin, N. V. C., and Boon, T. W. (2001).  
644 Weak cross-species relationships between body size and trophic level belie  
645 powerful size-based trophic structuring in fish communities. *Journal of*  
646 *Animal Ecology*, 70:934–944.
- 647 Jørgensen, C., Enberg, K., Dunlop, E. S., Arlinghaus, R., Boukal, D. S.,  
648 Brander, K., Ernande, B., Gårdmark, A., Johnston, F., Matsumura, S.,  
649 Pardoe, H., Raab, K., Silva, A., Vainikka, A., Dieckmann, U., Heino, M.,  
650 and Rijnsdorp, A. D. (2007). Managing evolving fish stocks. *Science*,  
651 318:1247–1248. doi:10.1126/science.1148089.
- 652 Kisdi, É. and Geritz, S. A. H. (2010). Adaptive dynamics: a framework  
653 to model evolution in the ecological theatre. *Journal of Mathematical*  
654 *Biology*, 61:165–169. doi:10.1007/s00285-009-0300-9.
- 655 Kolding, J., Bundy, A., van Zwieten, P. A. M., and Plank, M. J. (2016a).  
656 Fisheries, the inverted food pyramid. *ICES Journal of Marine Science*,  
657 73:1697–1713. doi:10.1093/icesjms/fsv225.
- 658 Kolding, J., Jacobsen, N. S., Andersen, K. H., and van Zwieten, P. A. M.  
659 (2016b). Maximizing fisheries yields while maintaining community struc-  
660 ture. *Canadian Journal of Fisheries and Aquatic Sciences*, 73:644–655.  
661 doi:10.1139/cjfas-2015-0098.
- 662 Law, R. (2007). Fisheries-induced evolution: present status and future  
663 directions. *Marine Ecology Progress Series*, 335:271–277.
- 664 Law, R., Kolding, J., and Plank, M. J. (2015). Squaring the circle: recon-  
665 ciling fishing and conservation of aquatic ecosystems. *Fish and Fisheries*,  
666 16:160–174. doi:10.1111/faf.12056.
- 667 Law, R., Plank, M. J., and Kolding, J. (2012). On balanced exploitation  
668 of marine ecosystems: results from dynamic size spectra. *ICES Journal*  
669 *of Marine Science*, 69:602–614. doi:10.1093/icesjms/fss031.

- 670 Law, R., Plank, M. J., and Kolding, J. (2016). Balanced exploitation  
671 and coexistence of interacting, size-structured, fish species. *Fish and*  
672 *Fisheries*, 17:281–302. doi:10.1111/faf.12098.
- 673 Metz, J. A. J., Geritz, S. A., Meszéna, G., Jacobs, F. J., and Heerwaarden,  
674 J. V. (1996). Adaptive dynamics, a geometrical study of the consequences  
675 of nearly faithful reproduction. In van Strien, S. J. and Verduyn Lunel,  
676 S. M., editors, *Stochastic and Spatial Structures of Dynamical Systems*,  
677 pages 183–231. North-Holland Publishing Co, Amsterdam, The Nether-  
678 lands.
- 679 Metz, J. A. J., Nisbet, R. M., and Geritz, S. A. H. (1992). How should  
680 we define fitness for general ecological scenarios? *Trends in Ecology and*  
681 *Evolution*, 7:198–202. doi.org/10.1016/0169-5347(92)90073-K.
- 682 Silvert, W. and Platt, T. (1978). Energy flux in the pelagic ecosystem: a  
683 time-dependent equation. *Limnology and Oceanography*, 23:813–816.
- 684 Sinko, J. W. and Streiffer, W. (1971). A model for populations reproducing  
685 by fission. *Ecology*, 52:330–335.
- 686 Smith, J. M. and Price, G. (1973). The logic of animal conflict. *Nature*,  
687 246:15–18.
- 688 Tillotson, M. D. and Quinn, T. P. (2018). Selection on the timing of  
689 migration and breeding: a neglected aspect of fishing-induced evolution  
690 and trait change. *Fish and Fisheries*, 19:170–181. doi:10.1111/faf.12248.
- 691 van Wijk, S. J., Taylor, M. I., Creer, S., Dreyer, C., Rodrigues, F. M.,  
692 Ramnarine, I. W., van Oosterhout, C., and Carvalho, R. (2013). Exper-  
693 imental harvesting of fish populations drives genetically based shifts in  
694 body size and maturation. *Frontiers in Ecology and the Environment*,  
695 11:181–187. doi:10.1890/120229.
- 696 Williams, G. C. (1966). *Adaptation and Natural Selection*. Princeton Uni-  
697 versity Press Princeton.
- 698 Zimmermann, F. and Jørgensen, C. (2017). Taking animal breeding  
699 into the wild: regulation of fishing gear can make fish stocks evolve  
700 higher productivity. *Marine Ecology Progress series*, 563:185–195.  
701 doi:10.3354/meps11996.

Table 1: Model parameters and values.

Parameter	Mackerel	Cod	Unit	Comments
<i>Fish life histories:</i>				
$w_0 e^{x_{i,0}}$	0.001	0.001	g	mass of fish egg
$w_0 e^{x_{i,m}}$	200	evolving	g	mass at 50% maturity
$w_0 e^{x_{i,\infty}}$	650	evolving	g	asymptotic mass
$\rho_{i,m}$	15	8	—	controls the body-size range over which maturation occurs
$\rho$	0.2	0.2	—	exponent for approach to asymptotic body size in reproduction function
<i>Dynamic size spectra of fish species:</i>				
$K$	0.2	0.2	—	food conversion efficiency
$\alpha_i$	0.8	0.8	—	search rate scaling exponent
$A_i$	750	700	$\text{m}^3 \text{yr}^{-1} \text{g}^{-\alpha}$	feeding rate constant
$\beta_i$	6	4.5	—	natural log of mean predator prey mass ratio
$\sigma_i$	2.5	1.9	—	diet breadth
$\mu_{o,i}^{(0)}$	0.1	0.1	$\text{yr}^{-1}$	intrinsic mortality rate at birth
$\xi$	-0.15	-0.15	—	exponent for intrinsic mortality
<i>Fixed plankton size spectrum:</i>				
$w_0 e^{x_{0,min}}$	$4.8 \times 10^{-11}$		g	lowest body mass of plankton
$w_0 e^{x_{0,max}}$	0.03		g	greatest body mass of plankton
$u_{0,0}$	100		$\text{m}^{-3}$	plankton density at 1 mg
$\gamma$	2		—	exponent of plankton spectrum



## 703 Figure legends

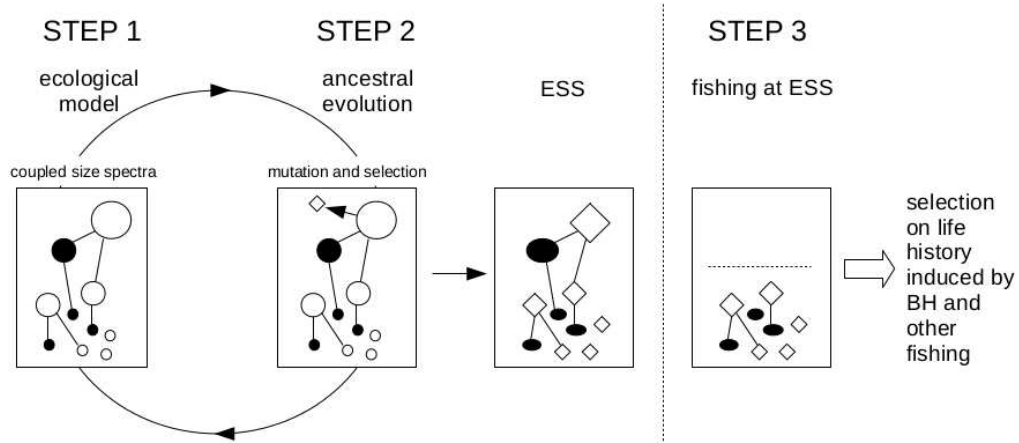


Figure 1: Road map of modelling steps. Boxes are cartoons of size spectra; with two species (filled and empty), and shapes depicting different phenotypes. The ecological model is run to determine the equilibrium state of the two species (STEP 1). New phenotypes are generated by mutation (STEP 2). The fate of a new phenotype is decided by the ecological dynamics (STEP 1). These steps are iterated as shown by the arrows until eventually the system reaches a state at which no further mutant can invade, an evolutionarily stable state (ESS). Contemporary fishing at this ancestral ESS generates new selection on the life history (STEP 3). The paper contrasts the strength of selection generated by balanced harvesting (BH) with size-at-entry and slot fishing.

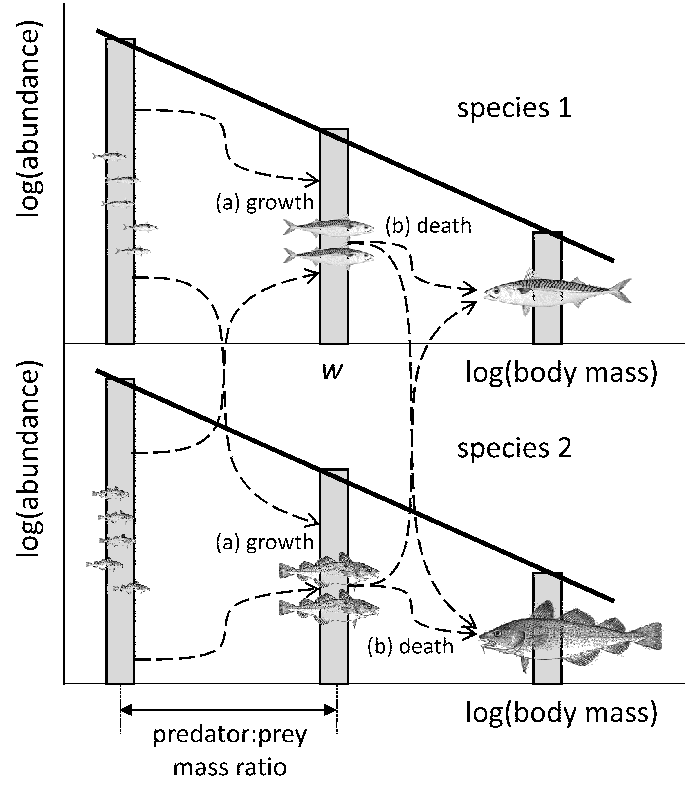


Figure 2: Processes acting on fish of body mass  $w$ . Growth comes from feeding on smaller fish of the same and other species, given by rate term (a) in Eq. (2.1). The main cause of death is predation and cannibalism by larger fish, a component of the rate term (b) in Eq. (2.1). Feeding is set by a preference function for prey relative to size  $w$ , determined by a species-specific predator:prey mass ratio. Heavy lines are examples of size spectra on log-log axes; these lines can change in shape over the course of time, as fish grow and die. Dashed lines show biomass flows from prey to predator.

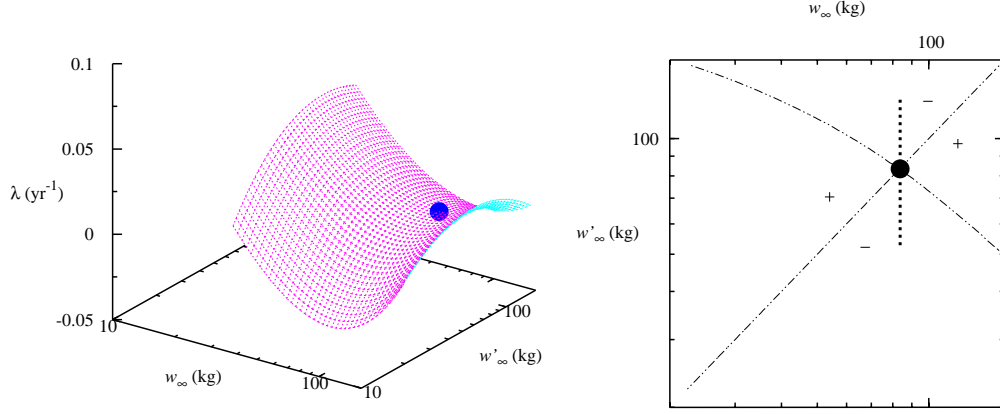


Figure 3: An example of an invasion fitness surface  $\lambda$  for a mutant with trait value  $w'_\infty$  as it enters a resident population with trait value  $w_\infty$ , and its corresponding pairwise invasibility plot (PIP), the section through the surface at  $\lambda = 0$ . Filled circles mark the singular point of evolution,  $w_\infty^*$ . Signs show the sectors of the PIP in which the invasion fitness of mutants is positive and negative, with boundaries given by the dash-dot line. The dotted line shows the direction in which selection gradient, Eq. (2.3), is measured.

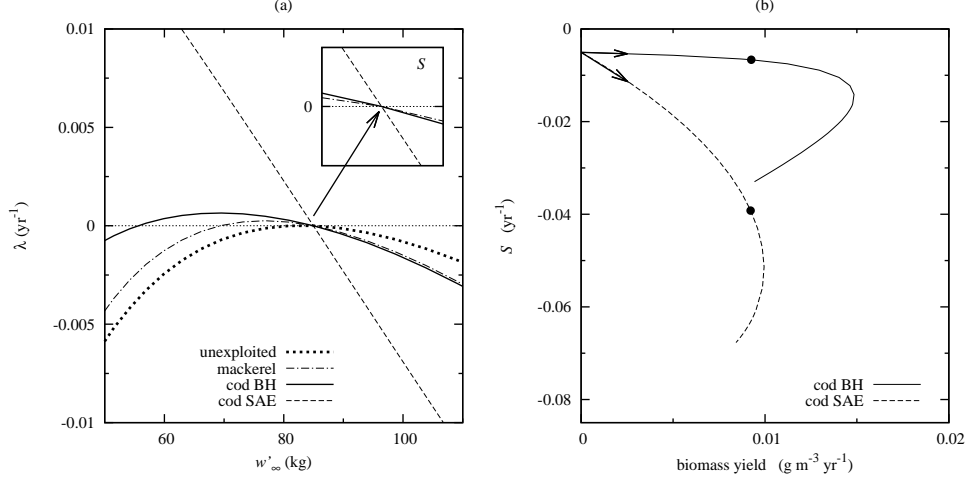


Figure 4: Invasion fitnesses and selection gradients  $S$  of cod mutants, under fishing schemes defined in the text. (a) Sections through invasion-fitness surfaces  $\lambda$  in the mutant direction  $w'_\infty$  at  $w_\infty^*$  (the direction of the dotted line in Fig. 3). The ancestral, unexploited system has a singular point of evolution  $w_\infty^*$  at 85 kg ( $S = 0$ ). The selection gradient on cod from fishing is measured by the gradient  $S$  at  $w_\infty^*$ , Eq. (2.3), as shown in the inset. Fishing mackerel, and not cod, leads to some selection on cod:  $S = -0.0051$  yr<sup>-1</sup>. Adding balanced harvesting (BH) on cod to the background fishing of mackerel, slightly increases selection on cod:  $S = -0.0067$  yr<sup>-1</sup> (cod minimum capture size 100 g,  $c = 11.0$  m<sup>3</sup> g<sup>-1</sup>). Adding size-at-entry (SAE) fishing on cod to the background fishing of mackerel, gives much stronger selection on cod:  $S = -0.0392$  yr<sup>-1</sup> (cod minimum capture size 1 kg,  $F = 0.2$  yr<sup>-1</sup>). (b) Effects of increasing cod fishing on selection gradients  $S$  and biomass yields (minimum capture sizes remain as in (a)). Arrows show the direction of increasing fishing on cod, starting from 0 and ending close to extinction of cod (near  $c = 70$  m<sup>3</sup> kg<sup>-1</sup> in the case of BH, and  $F = 0.32$  yr<sup>-1</sup> in the case of SAE). Filled circles mark the selection gradients of the cod BH and SAE fisheries shown in panel (a).

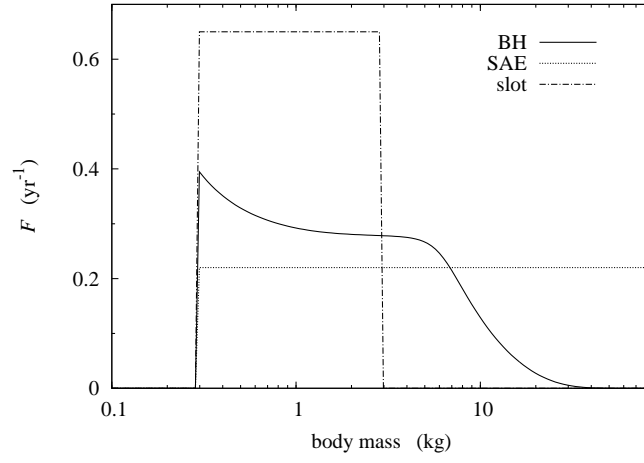


Figure 5: Three kinds of fishing mortality  $F$ : balanced harvesting (BH), size-at-entry (SAE), and slot. Each fishing pattern has a parameter controlling the overall fishing intensity, which moves the fishing mortality rates up or down; here their values are: BH  $c = 30 \text{ m}^3 \text{ g}^{-1}$ , SAE  $F = 0.22 \text{ yr}^{-1}$ , slot  $F = 0.65 \text{ yr}^{-1}$ . These parameter values were chosen to generate biomass yields near to  $0.01 \text{ g m}^{-3} \text{ yr}^{-1}$  at steady state. They give selection gradients  $S \text{ (yr}^{-1}\text{)}$ : BH  $-0.008$ , SAE  $-0.045$ , slot  $-0.014$ .

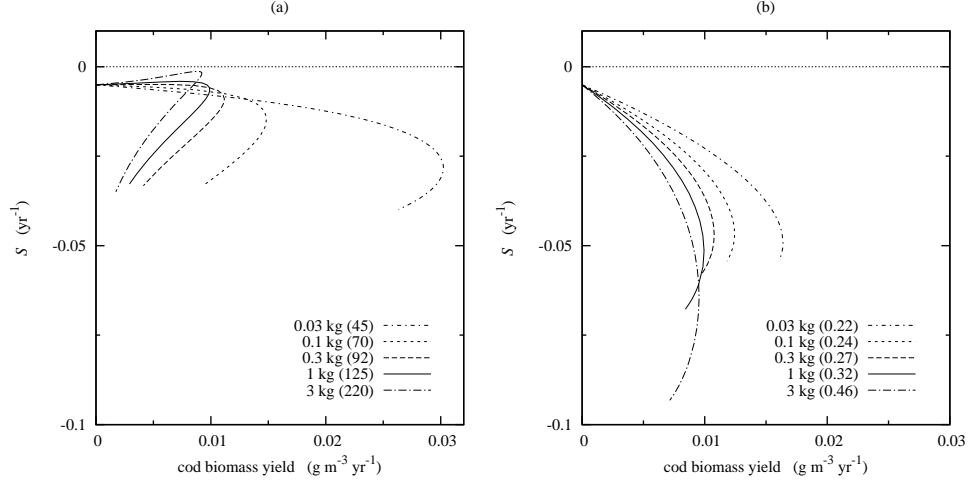


Figure 6: Selection gradients  $S$  and biomass yields of cod as fishing mortality on cod increases in: (a) balanced harvesting (BH) fisheries; (b) size-at-entry (SAE) fisheries. Each line describes a different minimum capture size, as shown in the keys. Lines end where fishing mortality rate causes extinction of cod; this is close to the value given in brackets,  $c$  ( $\text{m}^3 \text{kg}^{-1}$ ) in the case of BH, and  $F$  ( $\text{yr}^{-1}$ ) in the case of SAE.

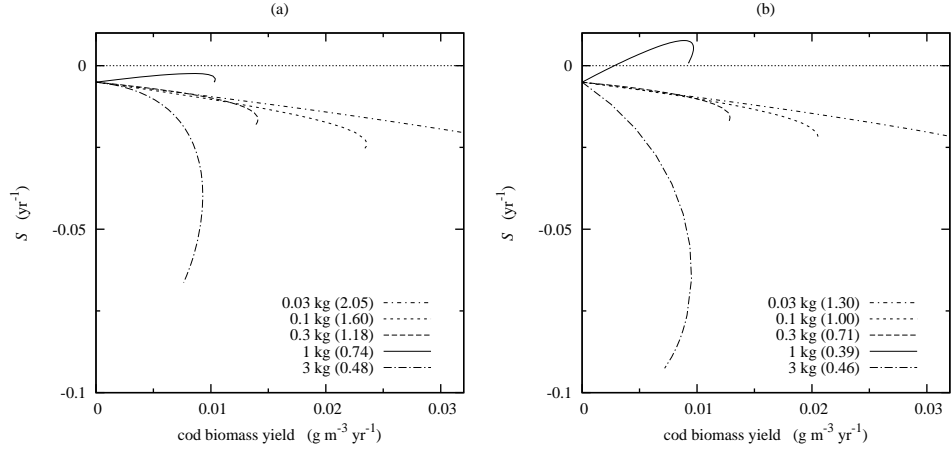


Figure 7: Selection gradients  $S$  and biomass yields of cod obtained as fishing mortality on cod increases in slot fisheries: (a) maximum capture size at 5 times the minimum; (b) maximum capture size at 10 times the minimum. Each line describes a different minimum capture size, as shown in the keys. Lines end where fishing mortality rate  $F$  causes extinction of cod close to the value ( $\text{yr}^{-1}$ ) given in brackets, except for minimum capture size 30 g, which is off the scale.

# Appendices

## A Multispecies dynamics

706 It is convenient to work in terms of the logarithmic body mass variable,  
 707  $x = \ln(w/w_0)$ , where  $w_0$  is an arbitrary body mass. This gives a state  
 708 variable  $u_i(x, t)dx = \phi_i(w, t)dw$ , with dimensions  $L^{-3}$ , which corresponds  
 709 to the density of individuals of type  $i$  with log body mass in the range  
 710  $[x, x + dx]$  at time  $t$ . ‘Type’ may be a species or a mutant within a species.  
 711 The dynamics of  $u_i(x)$  are given by the partial differential equation (Law  
 712 et al., 2016):

$$713 \quad \frac{\partial u_i}{\partial t} = \overbrace{-\frac{\partial}{\partial x} [\epsilon_i g_i u_i]}^{\text{growth}} + \overbrace{\frac{1}{2} \frac{\partial}{\partial x} \left[ e^{-x} \frac{\partial}{\partial x} [\epsilon_i G_i u_i] \right]}^{\text{diffusion}} + \overbrace{\frac{b_i R_i}{2} e^{-x}}^{\text{reproduction}} - \overbrace{\mu_{\text{tot}, i} u_i}^{\text{mortality}}, \quad (\text{A.1})$$

714 where the arguments  $x$  and  $t$  have been omitted from each function. The  
 715 functions  $g_i(x, t)$ ,  $G_i(x, t)$  and  $\mu_{\text{tot}, i}(x, t)$  respectively represent the rates of  
 716 mass-specific prey biomass assimilation, diffusion and mortality for type  $i$   
 717 at log body mass  $x$  and time  $t$ . The function  $R_i(t)$  is the reproduction rate  
 718 (number of eggs produced per unit volume per unit time) of type  $i$  at time  
 719  $t$ . The function  $\epsilon_i(x)$  is the proportion of assimilated prey biomass that is  
 720 used for somatic growth by individuals of type  $i$  and log body mass  $x$ . Each  
 721 of these functions will be defined below. The function  $b_i(x)$  represents the  
 722 mass distribution of eggs of type  $i$ . This is assumed to be a Dirac-delta  
 723 function, corresponding to a unique log mass  $x_{i,0}$  for type  $i$ . Eq. (A.1) is an  
 724 extension of the size-based McKendrick–von Foerster equation to include  
 725 a second-order diffusion-like term. This allows for demographic variability  
 726 in size-at-age trajectories (Datta et al., 2010, 2011), although in practice  
 727 this is small.

728 The model assumes that a predator of type  $i$  and log body mass  $x$   
 729 searches a volume of water  $A_i e^{\alpha_i x}$  per unit time, and has a relative pref-  
 730 erence for prey that is given by a function  $s_i(r)$  of the predator:prey mass  
 731 ratio  $r$ . The relative encounter rate between individuals of type  $i$  and indi-  
 732 viduals of type  $j$  is denoted  $\theta_{ij}$ . The mass-specific prey biomass assimilation  
 733 rate  $g_i(x)$  is calculated as an integral over the abundance of potential prey:

$$734 \quad g_i(x) = A_i K e^{(\alpha_i - 1)x} \sum_{j=0}^n \theta_{ij} \int e^{x'} s_i(e^{x-x'}) u_j(x') dx'. \quad (\text{A.2})$$

735 Similarly, the rate function for the second-order diffusion term  $G_i(x)$  is



736 given by (Law et al., 2016)

$$737 \quad G_i(x) = A_i K^2 e^{(\alpha_i - 1)x} \sum_{j=0}^n \theta_{ij} \int e^{2x'} s_i(e^{x-x'}) u_j(x') dx'. \quad (\text{A.3})$$

738 Three sources of mortality are included: predation mortality, natural  
739 non-predation mortality (referred to as intrinsic mortality) and fishing mor-  
740 tality

$$741 \quad \mu_{\text{tot},i}(x) = \mu_i(x) + \mu_{o,i}(x) + \mu_{F,i}(x).$$

742 The predation mortality rate  $\mu_i(x)$  is calculated as an integral over the  
743 abundance of potential predators:

$$744 \quad \mu_i(x) = \sum_{j=1}^n A_j \theta_{ji} \int e^{\alpha_j x'} s_j(e^{x'-x}) u_j(x') dx'. \quad (\text{A.4})$$

745 The intrinsic mortality rate  $\mu_{o,i}(x)$  accounts for sources of mortality other  
746 than predation and fishing. We assume that this is proportional to the  
747 mass-specific needs for metabolism, relative to the mass-specific rate at  
748 which food becomes available at size  $x$ . These rates are set relative to their  
749 values at egg size, so  $\mu_{o,i}(x_{i,0}) = \mu_{o,i}^{(0)}$  is a fixed baseline intrinsic mortality at  
750 birth for type  $i$ . The metabolic need should scale with body mass, and we  
751 write this as  $\exp(-\xi(x - x_{i,0}))$ , using the same exponent for all types. The  
752 mass-specific prey intake rate at size  $x$  relative to size  $x_{i,0}$  is  $g_i(x)/g_i(x_{i,0})$ .  
753 Thus

$$754 \quad \mu_{o,i}(x) = \mu_{o,i}^{(0)} \exp(-\xi(x - x_{i,0})) g_i(x_{i,0})/g_i(x), \quad (\text{A.5})$$

755 which is also a function of time because it depends on the mass-specific  
756 prey intake rate  $g_i(x)$ .

757 The feeding kernel for type  $i$  is a Gaussian function of log predator-to-  
758 prey mass ratio  $r$ , with mean  $\beta_i$  and standard deviation  $\sigma_i$ . The feeding  
759 kernel is assumed to be 0 when  $r < 1$  so that predators are always larger  
760 than their prey:

$$761 \quad s_i(r) = \begin{cases} \frac{1}{\sigma\sqrt{2\pi}} \exp\left(-\frac{(\ln(r)-\beta_i)^2}{2\sigma_i^2}\right) & r \geq 1 \\ 0 & r < 1 \end{cases}. \quad (\text{A.6})$$

762 The function  $\epsilon_i(x)$  the proportion of incoming prey biomass that is al-  
763 located to reproduction, using a form suggested by Hartvig et al. (2011):

$$764 \quad 1 - \epsilon_i(x) = [1 + \exp(-\rho_{i,m}(x - x_{i,m}))]^{-1} \exp(\rho(x - x_{i,\infty})). \quad (\text{A.7})$$

765 Here  $w_0 e^{x_{i,m}}$  is the body mass at which 50 % of the fish of type  $i$  are mature,  
766 and  $\rho_{i,m}$  defines the body-mass range over which fish are maturing. The

767 asymptotic body mass  $w_0 e^{x_{i,\infty}}$  is the size at which all incoming mass is  
 768 allocated to reproduction and no further somatic growth is possible, the  
 769 approach to this size being scaled by a parameter  $\rho$  common to all types.

770 The egg size  $x_{i,0}$  and asymptotic size  $x_{i,\infty}$  together give boundary condi-  
 771 tions for Eq. (A.1), over which there is no flux of individuals. For simplicity,  
 772 we do not deal with the dynamics of the plankton. This can be thought  
 773 of as an assumption that the plankton operate on a short timescale rel-  
 774 ative to the fish community. The fixed plankton spectrum was taken as  
 775  $u_0(x) = u_{0,0} \exp^{(1-\gamma)x}$ , where  $u_{0,0}$  is the abundance of plankton of mass 1  
 776 mg, giving a power-law relationship between body mass and abundance.  
 777 Parameter values are given in Table 1.

## 778 B Invasion fitness

779 We consider a resident community consisting of two species coexisting at  
 780 a stable equilibrium (though the following easily generalises to more than  
 781 two species). The discretised version of the size-spectrum model consists of  
 782 the abundance  $u_i$  of each species in size classes  $x_k$  ( $k = 1, \dots, N$ ) with step  
 783 size  $\Delta x$ . The Jacobian matrix of the two-species system takes the form

$$784 \quad \mathbf{J}_{\text{res}} = \begin{bmatrix} \mathbf{J}_{11} & \mathbf{J}_{12} \\ \mathbf{J}_{21} & \mathbf{J}_{22} \end{bmatrix}$$

785 where  $\mathbf{J}_{ij}$  is the  $N \times N$  matrix describing the dependence of species  $i$  on  
 786 species  $j$ . We require that this two-species system has a stable equilibrium  
 787 in which both species are non-zero, so that all eigenvalues of the Jacobian  
 788 evaluated at this equilibrium,  $\mathbf{J}_{\text{res}}^*$ , have negative real part.

789 Now suppose the community is augmented by a mutant of species 2  
 790 indexed  $2'$ . The expanded system has a Jacobian matrix of the form

$$791 \quad \mathbf{J}_{\text{aug}} = \begin{bmatrix} \mathbf{J}_{11} & \mathbf{J}_{12} & \mathbf{J}_{12'} \\ \mathbf{J}_{21} & \mathbf{J}_{22} & \mathbf{J}_{22'} \\ \mathbf{J}_{2'1} & \mathbf{J}_{2'2} & \mathbf{J}_{2'2'} \end{bmatrix}.$$

792 The state at which the resident species 1 and 2 are at the two-species equi-  
 793 librium and the mutant  $2'$  is absent is also an equilibrium of the augmented  
 794 system. When the Jacobian matrix  $\mathbf{J}_{\text{aug}}$  is evaluated at this equilibrium,  
 795 the submatrices  $\mathbf{J}_{2'1}$  and  $\mathbf{J}_{2'2}$  are zero. Hence the Jacobian is

$$796 \quad \mathbf{J}_{\text{aug}}^* = \begin{bmatrix} \mathbf{J}_{11} & \mathbf{J}_{12} & \mathbf{J}_{12'} \\ \mathbf{J}_{21} & \mathbf{J}_{22} & \mathbf{J}_{22'} \\ 0 & 0 & \mathbf{J}_{2'2'}^* \end{bmatrix} \quad (\text{B.1})$$

797 The eigenvalues of this matrix consist of the eigenvalues of  $\mathbf{J}_{\text{res}}^*$ , which all  
 798 have negative real part, together with the eigenvalues of  $\mathbf{J}_{2'2'}^*$ , which is  $\mathbf{J}_{2'2'}$   
 799 evaluated at the coexistence equilibrium of 1 and 2, with  $2'$  at zero.

800 The elements of the Jacobian  $\mathbf{J}_{2'2'}$  can be obtained from the discretised  
 801 version of the PDE, Eq. (A.1), for the mutant. For brevity, we drop the  
 802 mutant index by using  $u_k$  to denote  $u_{2'}(x_k)$ , and similarly  $g_k$ ,  $G_k$ ,  $\epsilon_k$ ,  $\mu_{\text{tot},k}$ .  
 803 The discretised version of the PDE is then:

$$\begin{aligned}
 \frac{du_k}{dt} = & \frac{\epsilon_{k-1}g_{k-1}u_{k-1} - \epsilon_k g_k u_k}{\Delta x} \\
 & + e^{-x_k} \frac{\epsilon_{k-1}G_{k-1}u_{k-1} + \epsilon_{k+1}G_{k+1}u_{k+1} - 2\epsilon_k G_k u_k}{2\Delta x^2} \\
 & + e^{-x_k} \frac{\epsilon_{k-1}G_{k-1}u_{k-1} - \epsilon_k G_k u_k}{2\Delta x} \\
 & - \mu_{\text{tot},k}u_k + \frac{\delta_{k1}Re^{-x_0}}{\Delta x},
 \end{aligned} \tag{B.2}$$

808 where  $\delta_{kl}$  is the Kronecker-delta symbol.

809 From Eq. (B.2), the elements of  $\mathbf{J}_{2'2'}^*$  are:

$$\begin{aligned}
 a_{kk} &= -\frac{\epsilon_k g_k}{\Delta x} - e^{-x_k} \epsilon_k G_k \left( \frac{1}{\Delta x^2} + \frac{1}{2\Delta x} \right) - \mu_{\text{tot},k}, \\
 a_{k,k-1} &= \frac{\epsilon_{k-1}g_{k-1}}{\Delta x} + e^{-x_k} \epsilon_{k-1}G_{k-1} \left( \frac{1}{2\Delta x^2} + \frac{1}{2\Delta x} \right), \\
 a_{k,k+1} &= \frac{e^{-x_k} \epsilon_{k+1}G_{k+1}}{2\Delta x^2}, \\
 a_{1k} &= \frac{e^{x_k-x_0}(1-\epsilon_k)g_k}{2}.
 \end{aligned} \tag{B.3}$$

814 All other elements of  $\mathbf{J}_{2'2'}^*$  are zero because terms of the form  $\partial/\partial u_l(g_k u_k)$   
 815 are all zero when evaluated at the equilibrium  $u_k = 0$ . The functions  $g_k$ ,  
 816  $G_k$  and  $\mu_{\text{tot},k}$  depend on the resident abundances via Eqs. (A.2)–(A.4).  
 817 In the special case considered in this model, where the only difference  
 818 between the mutant  $2'$  and the resident 2 is in its reproduction schedule  
 819 ( $\epsilon_k$ ), the functions  $g_k$ ,  $G_k$  and  $\mu_{\text{tot},k}$  will be identical to those for the resident  
 820 2. In other words, the mutant experiences the same size-dependent food  
 821 intake and mortality rates as the resident, but differs in the proportion of  
 822 incoming biomass that is allocated to reproduction. In the simpler case  
 823 of the McKendrick—von Foerster equation without diffusion, the Jacobian  
 824 elements above omit all terms containing  $G_k$ .

825 The two-species coexistence equilibrium is stable to introduction of the  
826 mutant (i.e. a rare mutant will die out) if all eigenvalues of  $\mathbf{J}_{2',2'}^*$  have  
827 negative real part. If  $\mathbf{J}_{2',2'}^*$  has an eigenvalue with positive real part, the  
828 two-species equilibrium is unstable to the introduction of the mutant (i.e.  
829 a rare mutant will increase in abundance). The eigenvalue with largest real  
830 part  $\lambda$  is the rate of increase of the mutant population when the mutant is  
831 rare, i.e. the invasion fitness.

## 832 C Numerical methods

833 We took a community of two fish species, one growing to a small size, and  
834 the other to a large size, together with a fixed plankton spectrum. This  
835 was based on Law et al. (2016), the two species having parameter values  
836 motivated by mackerel and cod (Table 1) as described in Law et al. (2016).  
837 The dynamics were described by Eqns (A.1), with mackerel indexed  $i = 1$ ,  
838 and cod  $i = 2$ . The asymptotic body mass of cod,  $x_\infty = \ln(w_\infty)$ , was set to  
839 evolve, and the mass at 50 % maturation,  $x_m = \ln(w_m)$ , evolved with it as  
840 fixed proportion  $\ln(1/15)$  of this. The matrix of preferences  $\theta_{ij}$  of predators  
841 of type  $i$  for prey of type  $j$  was:

$$842 \quad \boldsymbol{\theta} = \begin{pmatrix} 0 & 0 & 0 & 0 \\ 1 & 1 & 0.2 & 0.2 \\ 1 & 0.2 & 1 & 1 \\ 1 & 0.2 & 1 & 1 \end{pmatrix}. \quad (\text{C.1})$$

843 The first three rows of  $\boldsymbol{\theta}$ , indexed  $i = 0, 1, 2$ , refer respectively to: (0)  
844 plankton, (1) mackerel, and (2) cod with resident trait value  $x_\infty$ . The final  
845 row refers to predation by mutant cod  $x'_\infty$ , with predation preferences set  
846 to be the same as resident cod. The cross-species predation parameters,  
847  $\theta_{ij} = 0.2$ , were chosen to take cod's  $x_\infty$  to a singular point of ancestral  
848 evolution  $x_\infty^*$  near that of the largest recorded cod.

849 TABLE 1 NEAR HERE

850 For numerical analysis, the continuous equations were discretized to  
851 a system of ordinary differential equations using as small a step size as  
852 practicable ( $\Delta x = 0.05$ ). For given parameter values, we obtained a close  
853 approximation to the steady state from a numerical integration over a 100  
854 yr time period, using a time step  $\Delta t = 0.0005$ , based on the Euler method.  
855 The Gaussian feeding kernel  $s_i(r)$  Eq. (A.6) was truncated at  $\pm 3\sigma$ , and  
856 normalised to sum to 1. Fast Fourier transforms were used to compute  
857 the convolution integrals. In cases where convergence to the steady state  
858 was slow, the time period of integration was extended. We terminated  
859 sequences of increasing fishing mortality at extinction of the cod.

860 Having reached the steady state of an arbitrary resident community  
 861 (with cod's trait value at  $x_\infty$ ), we constructed the life history of a rare mu-  
 862 tant with an altered trait value  $x'_\infty$ . The Jacobian matrix of the resident  
 863 community, augmented by the rare mutant, could then be built, with ele-  
 864 ments as given in Eqs (B.3). The invasion fitness,  $\lambda(x'_\infty, x_\infty)$ , of the mutant  
 865 cod in the resident community is the real part of the leading eigenvalue of  
 866 this matrix.

867 A singular point of evolution  $x_\infty^*$  occurs at

$$868 \quad 0 = \frac{\partial}{\partial x'_\infty} \lambda(x'_\infty, x_\infty) \Big|_{x'_\infty = x_\infty}, \quad (\text{C.2})$$

869 obtained numerically from a pairwise invasibility plot, using a grid of values  
 870  $(x'_\infty, x_\infty)$  of invasion fitness (Fig. 3). The strength of directional selection  
 871 generated by fishing on cod at the singular point  $x_\infty^*$ , was measured as

$$872 \quad S = \frac{\lambda(x'_\infty + \delta x, x_\infty^*) - \lambda(x'_\infty - \delta x, x_\infty^*)}{2\Delta x}. \quad (\text{C.3})$$

873 We checked the integrations by running two independently constructed  
 874 versions of the code. We also checked the eigenvalue measure of invasion  
 875 fitness by direct measurement of the rate of increase of rare mutants.

## 876 **D Fishing mortality under balanced harvest-** 877 **ing**

878 Balanced harvesting, as defined in this paper, sets the fishing mortality  
 879 rate on species  $i$  at time  $t$  in proportion to the current rate of somatic  
 880 production at each body mass  $x$ , from some minimum capture size  $x_{min}$   
 881 onwards. Production rate is measured as

$$882 \quad p_i(x, t) = \epsilon_i(x) g_i(x, t) u_i(x, t) w_0 e^x, \quad (\text{D.1})$$

883 where  $g_i(x, t)$  is the mass-specific assimilation rate of prey biomass Eq.  
 884 (A.2),  $\epsilon_i(x)$  is the proportion of this prey biomass allocated to somatic  
 885 growth,  $u_i(x, t)$  is the the density of individuals with log body mass in  
 886 the range  $[x, x + dx]$ , and  $w_0 e^x$  is the predator mass. This gives a fishing  
 887 mortality rate  $F_i(x, t)$

$$888 \quad F_i(x, t) = \begin{cases} 0 & \text{if } x < x_{min} \\ cp_i(x, t) & \text{if } x \geq x_{min} \end{cases}. \quad (\text{D.2})$$

889 Here  $c$  is a constant of proportionality with dimensions  $\text{vol. mass}^{-1}$  or  
890  $\text{area mass}^{-1}$ , and can be thought of as a mass-specific exploitation ratio.  
891 Production rate changes over time as the density functions  $u_i(x, t)$  change.  
892 Balanced harvesting tracks the changing production rate until the ecosys-  
893 tem reaches its ecological steady state. The calculations in this paper use  
894 the fishing mortalities at this steady state.